



Enhanced photocatalytic degradation of nigrosine dye from its aqueous solution using $\text{La}_2\text{Ce}_2\text{O}_7$ nanoparticles

Nutan Salvi¹, Rukhsar Banu¹, Chetna Ameta¹, Rakshit Ameta² & Pinki B Punjabi*¹

¹Photochemistry Laboratory, Department of Chemistry, University College of Science,
M. L. Sukhadia University, Udaipur 313002, Rajasthan, India

²Department of Chemistry, J.R.N. Rajasthan Vidyapeeth (Deemed to be University), Udaipur 313001, Rajasthan, India

E-mail: pb_punjabi@yahoo.com

Received 4 March 2020; accepted 23 February 2021

In the present work, removal of nigrosine dye from its aqueous solution via combined photocatalysis and adsorption has been reported using ternary catalyst lanthanum cerate under visible light. The catalyst has been synthesized by citric acid assisted sol-gel method. XRD graph reveals that the average crystallite size of sample is found to be approximate 4.0 nm having cubic fluorite structure. There is 64.45% oxygen, 17.76% lanthanum and 17.79% cerium atoms present in the material, as observed by EDS result. FESEM results shows that obtained particles are in the form of rice grain shape arranged densely in homogeneous manner. TGA curve shows that there is a evaporation of moisture, nitrate and carbon. Two exothermic peaks are observed at about 170°C and 200°C in the DTA curve. The UV-Visible spectrum gives the band gap of lanthanum cerate and it is 3.0 eV. A spectrophotometer has been used to follow the photocatalytic degradation of nigrosine dye at specific intervals of time. The effect of various parameters such as pH, concentration of dye, photocatalyst dosage and light intensity has been studied on the rate of degradation. A tentative mechanism for degradation of nigrosine has been proposed involving superoxide and hydroperoxyl radicals as main oxidizing species.

Keywords: Lanthanum cerate, Ternary, Nigrosine, Photocatalyst, Adsorption

Developments in industrial and agriculture sector have resulted in generation of large amount of waste water containing toxic pollutants. Organic dyes are one of the larger groups of pollutants which are released from textile industrial waste water. Some of the effects of dye bearing waste water are aesthetic pollution of environment and also carcinogenicity due to their degradation products. There are more than 100,000 varieties of dyes available in the market, which are used in the textile, cosmetics, food, paper, leather industries and pharmaceutical industries. About 10% of the total dyes used are lost as wastewater, which affect the environment by poisoning effects in living organisms¹⁻³. Various techniques including photocatalysis, chemical oxidation, coagulation, reverse osmosis, nano-filtration, adsorption etc., are used for the removal of dyes from waste water. Among these techniques adsorption and photocatalysis have been widely used as effective methods for dye removal from wastewater. Adsorption has been reported to be an economic process for the removal of colored pollutants from industrial effluents⁴. Advanced oxidation processes (AOPs) have become some of the most effective methods for the treatment of

polluted water containing organic pollutants, particularly low-biodegradable pollutants⁵⁻⁷. AOPs are able to complete mineralization of organic pollutants to carbon dioxide, water and inorganic compounds⁸⁻¹⁰. Heterogeneous photocatalysis, as one of the AOPs, is an effective method to oxidize most of the organic carbon at ambient conditions¹¹.

The photocatalytic activity of the La-doped BiFeO_3 catalyst was 3.4 times that of un-doped BiFeO_3 in the degradation of phenol under simulated sunlight irradiation for 180 minutes¹². A comparative study for the photocatalytic degradation of methylene blue dye has been investigated using undoped ZnO , mono-doped and La-Zr- ZnO photocatalysts. It was observed that the photocatalytic activity of the La-Zr- ZnO photocatalyst is much higher than that of undoped and mono-doped ZnO ¹³. The photocatalytic activity of La-doped ZnO was compared with the pure ZnO in the degradation of 2,4,6-trichlorophenol (TCP). The results showed that the rate of degradation of TCP for La-doped ZnO is much higher as compared to that of pure ZnO ¹⁴. Lanthanum-modified P25 TiO_2 catalysts were used in catalytic removal of

2,4-D herbicide, which is a commonly found as drinking water contaminant¹⁵. Wang *et al.* reported the use of La/Bi₂WO₆ as photocatalyst for the degradation of reactive brilliant red X-3B and rhodamine B under simulated solar irradiation¹⁶. Methylene blue, a widely used textile dye has been photocatalytically degraded in presence of LaCrO₄ as a photocatalyst¹⁷.

Now-a-days the importance of photocatalysis has increased for the degradation of pollutants present in effluents. From the literature survey, it has been observed that no attention has been paid on the use of lanthanum cerate as photocatalyst for the degradation of dyes. Therefore, in the present work, nano-sized photocatalyst lanthanum cerate has been prepared by sol-gel method and used for the degradation of nigrosine under visible light. It is an organic dye and highly soluble in water with black color solutions. It is an anionic dye. Nigrosine is employed as a common biological stain for tissues and cell. It is used in textile, plastic, shoe-polish and ink industries for dyeing purposes. The crude mixture containing nigrosine hydrochlorides is employed for dyeing phenolic resins. From the above literature survey, it can be assumed that the photocatalytic process could be an efficient method for removal of nigrosine dye from its aqueous solution with the advantages of less chemical requirement and short treatment period. The molecular weight of nigrosine (C₂₂H₁₄N₆Na₂O₉S₂) is 616.49 and its maximum wavelength of absorption is 570 nm.

Experimental Section

Materials

Lanthanum nitrate (Alfa Aesar 99.9%), cerium nitrate (Himedia), citric acid (Himedia) absolute alcohol and nigrosine (Himedia) were used in the present investigation. All the chemicals were of analytical grade and used without further purification.

Citric acid assisted synthesis of nanoparticles of lanthanum cerate (La₂Ce₂O₇)

For the synthesis of ternary photocatalyst, La(NO₃)₃.6H₂O (0.1M), Ce(NO₃)₃.6H₂O (0.1M) and citric acid (0.2M) were dissolved in 30 mL mixture of H₂O and EtOH (1:1) to yield a homogeneous solution. The solution was stirred on magnetic stirrer for 1 hour. The solution was stirred again at 70°C until it acquires homogeneous yellow coloured gel status. The gel is dried at 90°C for 24 h. The dried gel was grounded with the help of mortar and pestle. The grounded material was calcined at 600°C for 5 h with a heating rate of 2°C/min, and the final product was characterized by spectral analysis as La₂Ce₂O₇.

Citric acid forms chelate compounds with lanthanum and cerium. These complex ions are homogeneously distributed over the solution and during the gel formation, too. It also acted as a fuel during calcination. A white spongy mass obtained after calcination is grinded to give fine powder of La₂Ce₂O₇.

Results and Discussion

X-ray diffraction (XRD) method

Single phase formation of the ternary oxide is confirmed by X-ray diffraction technique. XRD of the sample was recorded on XPERT-PRO diffractometer with Cu K α radiations. The accelerating voltage and the applied current were 35 kV and 20 mA, respectively. Diffraction pattern was recorded over the 2 θ range from 10° to 90° with a step size of 0.017°. Figure 1 displays the XRD of nano-sized La₂Ce₂O₇ photocatalyst. Good intensity of the Bragg's peaks reflects well ordered crystalline structure and significant broadening in the Bragg's peaks indicate for nanocrystalline nature of the sample. The average crystallite size (*t*) is determined using the standard Scherrer's formula: $t = 0.94\lambda / \beta \cos \theta$ where λ is the wavelength of X-rays used (1.5406 Å), β

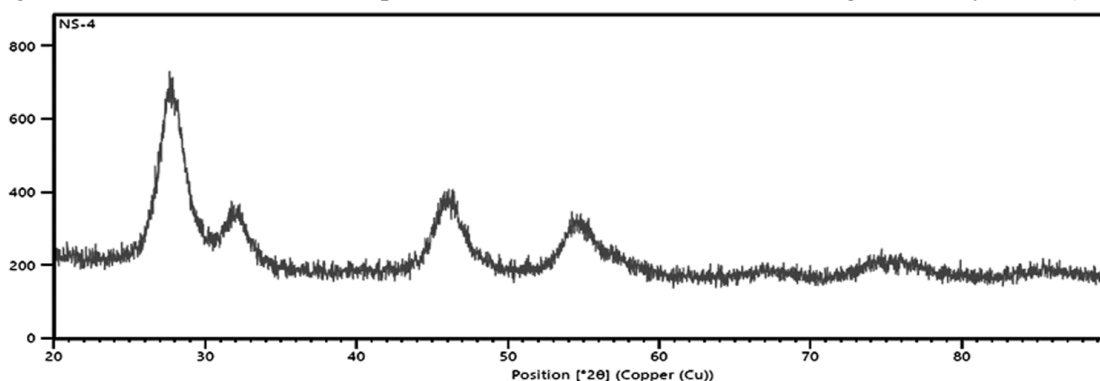


Fig. 1 – XRD pattern of La₂Ce₂O₇ nanoparticles

is the full width at half maximum (FWHM) and θ is the angle of diffraction. The average crystallite size (or average particle size for the reported sample) of sample is found to be approximate 4.0 nm for all diffraction peaks.

In the XRD pattern all the observed diffraction peaks matches with the cubic fluorite phase of CeO_2 (JCPDS file No. 01-089-8436) (Ref. 18). The diffraction peaks with 2 theta values at 28.12° , 32.42° , 46.62° and 55.81° can be well indexed to (111), (200), (220) and (311) planes of a cubic fluorite structure, respectively. These four intense peaks that correspond to the pure $\text{La}_2\text{Ce}_2\text{O}_7$ phase are also reported in the literature¹⁹⁻²². The obtained value of the cubic lattice parameter is found to be 5.567\AA . Furthermore, peaks corresponding to the individual

oxides (La_2O_3 etc.) were not observed indicating the formation of $\text{La}_2\text{Ce}_2\text{O}_7$ solid solution formation. No evidence of $\text{La}_2\text{Ce}_2\text{O}_7$ pyrochlore phase was observed.

Energy dispersive spectroscopic (EDS) analysis

EDS measurements were done for $\text{La}_2\text{Ce}_2\text{O}_7$ nanoparticles prepared by calcination of the as synthesized product at 600°C for 5 h as shown in Fig. 2. The results obtained in atomic percentage for sample shows the stoichiometric chemical composition as $\text{La}_2\text{Ce}_2\text{O}_7$. There is 64.45% oxygen, 17.76% lanthanum and 17.79% cerium atoms present in the material, as observed by EDS result.

Field emission scanning electron microscopy (FESEM)

FESEM images of synthesized $\text{La}_2\text{Ce}_2\text{O}_7$ nanoparticles have been shown in Fig. 3. It was

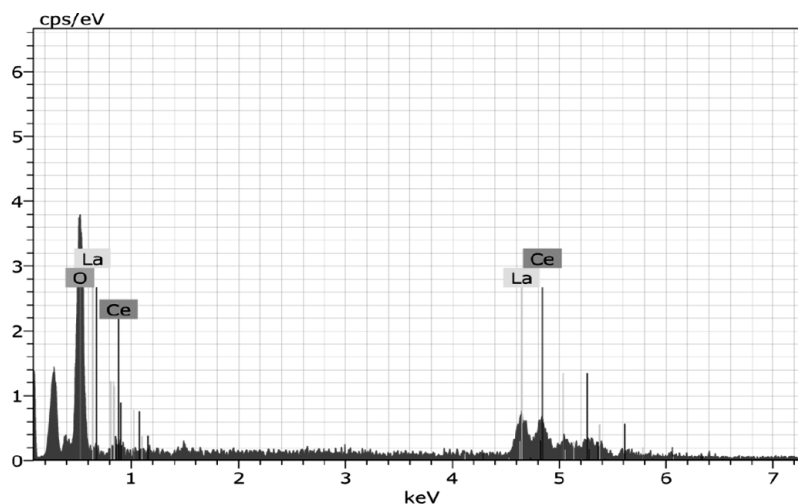


Fig. 2 – EDS spectrum of $\text{La}_2\text{Ce}_2\text{O}_7$

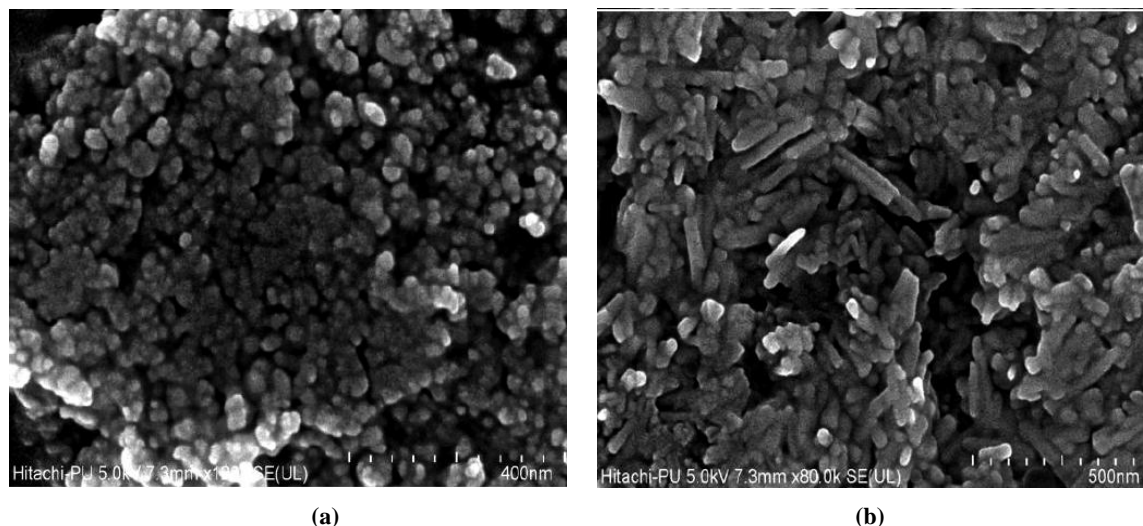


Fig. 3 – FESEM images of $\text{La}_2\text{Ce}_2\text{O}_7$ nanoparticles

recorded on cold field emission electron microscope, Hitachi PU8010. FESEM results give the direct information about the size and structure of the synthesized $\text{La}_2\text{Ce}_2\text{O}_7$ nanoparticles. The obtained particles are in the form of rice grain shape arranged densely in homogeneous manner. As shown in the Fig. 3 (a), it is clear that the diameter size of the grain shape nanoparticles is about 14-28 nm. In Fig. 3 (b) length size of rice like structure is 80-120 nm and thickness size is about 35-50 nm.

Transmission electron microscopy (TEM) analysis

TEM image was recorded by using Philips Tecnai 20. The morphology, particle size and structure of the synthesized $\text{La}_2\text{Ce}_2\text{O}_7$ were examined by TEM. Figure 4 illustrates the TEM image of the $\text{La}_2\text{Ce}_2\text{O}_7$, and the shape and size of particles resemble with the results obtained from XRD and FESEM.

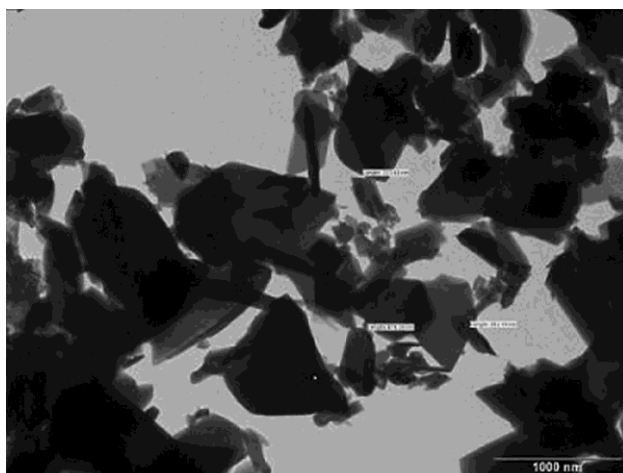


Fig. 4—TEM image of $\text{La}_2\text{Ce}_2\text{O}_7$

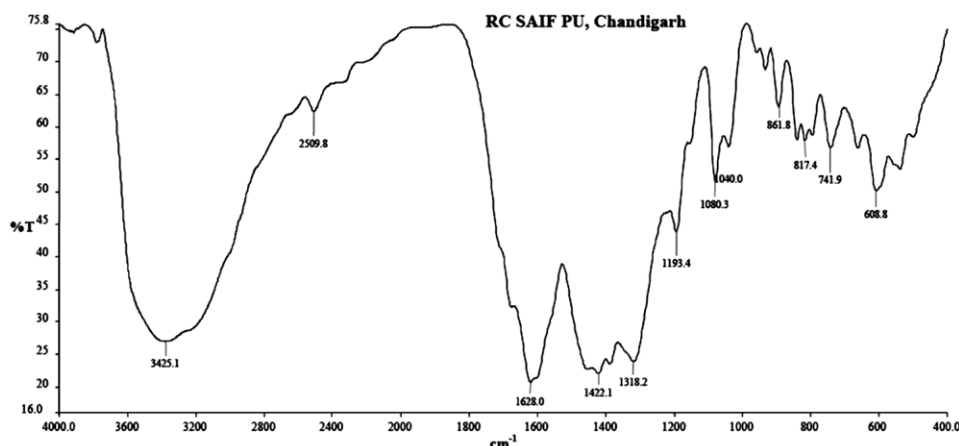


Fig. 5 — FTIR spectrum of $\text{La}_2\text{Ce}_2\text{O}_7$ nanoparticles

Fourier-transform infrared spectroscopy (FTIR) analysis

FTIR analysis was performed by using Perkin Elmer Spectrum RX-I FTIR. Figure 5 shows the FTIR spectrum of $\text{La}_2\text{Ce}_2\text{O}_7$ nanoparticles in the range 400-4000 cm^{-1} . Several characteristic absorption bands can be observed at about 608, 741, 817, 861, 1040, 1080, 1193, 1318, 1422, 1628, 2509, 3425 cm^{-1} . The intense signal detected at approximately 3400 cm^{-1} is an evidence for the presence of water molecules contained in the particles. The presence of the band near 3400 cm^{-1} in the spectra of the $\text{La}_2\text{Ce}_2\text{O}_7$ corresponds to the water molecule absorbed in the samples^{23,24}. In addition the band located at 1628 cm^{-1} represents another vibration of water molecule²⁵. Bands between 1600 and 1000 cm^{-1} indicate the presence of nitrates²⁶. A peak with very weak intensity at 861 cm^{-1} can be assigned to the residual nitrate ion²⁷.

Thermal gravimetry (TGA) and Differential thermal (DTA) analysis

Thermogravimetric analysis of the as-prepared sample was studied from room temperature to 700 °C at a heating rate of 20°C/min under nitrogen atmosphere having a flow rate of 20 mL/min. It was recorded on STA- 6000 (DTA-TGA) Perkin Elmer. Figure 6(a) shows that the weight loss occurs in two stages, first stage taking place from room temperature up to 100°C, the weight loss during first stage occurs due to the evaporation of moisture. The weight loss during second stage from temperature 100°C up to 200°C occurs due to evaporation of nitrate and carbon (from unreacted ethanol and citric acid). Above 200°C the sample is almost impurity free, which is observed from the graph. Figure 6(b) shows the DTA curve for as prepared sample. The two exothermic peaks at about 170°C and 200°C in the DTA curve correspond to the

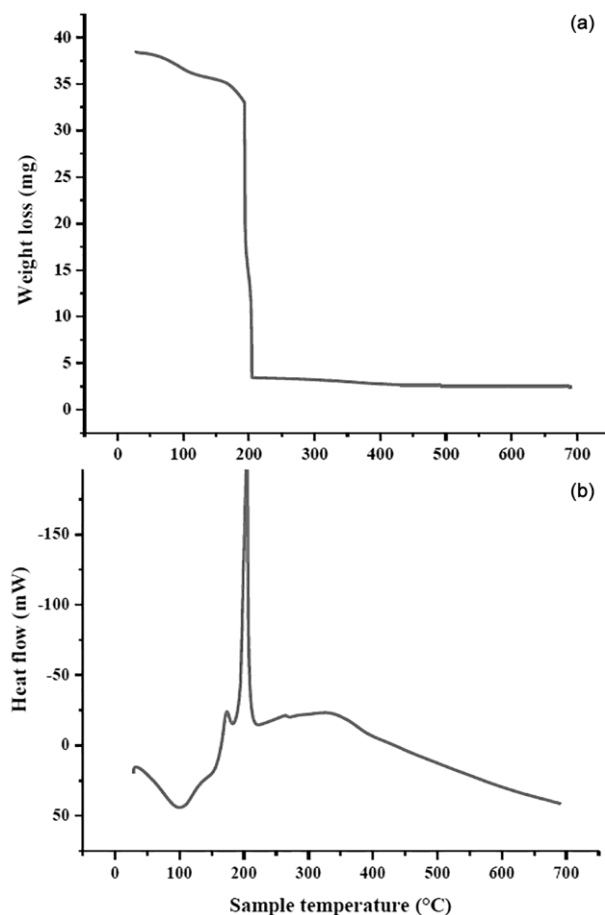


Fig. 6 – (a) TGA and (b) DTA curves of $\text{La}_2\text{Ce}_2\text{O}_7$

decomposition of unreacted citric acid and nitrates of lanthanum and cerium.

UV-Visible spectrum

UV-Visible spectrum of as-synthesized lanthanum cerate was recorded in wavelength range 200–800 nm using Perkin-Elmer Lambda-750 UV-visible spectrophotometer. The spectrum and its Tauc plot showing band gap are given in Fig. 7(a) and 7(b). The band gap of lanthanum cerate was calculated to be 3.0 eV.

Photocatalytic degradation of nigrosine

Lanthanum cerate as photocatalyst has been used for the degradation of nigrosine dye. Stock solution of nigrosine (1.0×10^{-3} M) was prepared in doubly distilled water. A reaction mixture containing dye ($\approx 10^{-5}$ M) and 0.08g photocatalyst was irradiated with a 200 W tungsten lamp (Philips). The progress of the dye degradation was monitored by measuring the absorbance of the reaction mixture at regular time intervals using UV-Vis spectrophotometer (Electronics India Model 2371) at 570 nm. The intensity of light

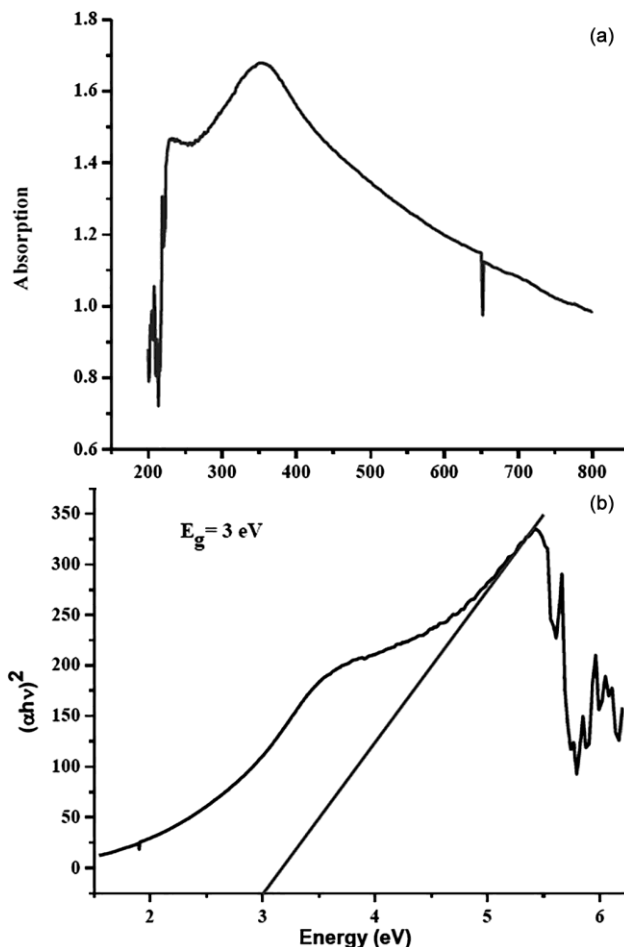


Fig. 7 – (a) UV-Visible spectrum of $\text{La}_2\text{Ce}_2\text{O}_7$ and (b) its Tauc plot

from the lamp was measured using a Solarimeter (SM CEL 201). A water filter was used to cut off thermal radiations. A digital pH meter (Systronics Model 335) was used to measure the pH of the reaction mixture. The pH of the solution was adjusted by the addition of previously standardized 0.1 N H_2SO_4 and 0.1 N NaOH solutions. Different quality parameters for polluted and treated water were determined by using water analyser (Systronics Model 371).

It was observed that the absorbance of the dye solution decreases with the increasing time of exposure, which indicates that the concentration of nigrosine dye decreases with increasing time. A plot of $2 + \log A$ versus time was linear following pseudo-first order kinetics. The rate constant was calculated with the expression : $k = 2.303 \times \text{slope}$. The results are tabulated in Table 1.

Effect of pH

The effect of pH on the rate of degradation has been investigated in pH range 5.0-9.0 keeping all

Table 1 – Typical run for photocatalytic degradation of nigrosine
 $pH = 8.0$ [Nigrosine] = 10×10^{-5} M Photocatalyst = 0.08 g Light
intensity = 60.0 mWcm^{-2}

Time (min.)	Absorbance	$2 + \log A$
0	0.799	1.903
10	0.701	1.846
20	0.548	1.739
30	0.459	1.662
40	0.376	1.576
50	0.287	1.458
60	0.219	1.341
70	0.194	1.289
80	0.161	1.207
90	0.125	1.098
100	0.107	1.033
110	0.094	0.976
120	0.072	0.859
Rate constant (k)		$3.38 \times 10^{-4} \text{ (sec}^{-1}\text{)}$

other parameters identical. The decrease in the rate of reaction on moving from pH 8.0 to 5.0 may be attributed to the formation of HO_2^\cdot radical on the reaction of $\text{O}_2^{\cdot-}$ radical with H^+ ion. Therefore, concentration of $\text{O}_2^{\cdot-}$ radical decreases. The HO_2^\cdot radical is less powerful reducing agent than $\text{O}_2^{\cdot-}$ radical. Therefore rate of reaction decreases on moving from 8.0 to 5.0. On the other hand rate also decreases on increasing the pH beyond 8.0. It is because the surface of catalyst becomes negatively charged in alkaline medium. The nigrosine dye is anionic in nature. There is an electrostatic repulsion between negatively charged photocatalyst surface and anionic dye, which hinders the approach of dye towards photocatalyst surface. This reason causes the retardation of rate beyond pH 8. The optimum pH for photocatalytic degradation of nigrosine was observed at pH 8.0.

Effect of concentration of dye

The effect of variation of concentration of nigrosine on its degradation rate has been observed in the range from 5×10^{-5} M – 13×10^{-5} M keeping all other parameters identical. It has been observed that the rate of degradation increases with increasing concentration of dye up to 10×10^{-5} M. Further increase in concentration beyond this limit results in a decrease in degradation rate. This can be explained on the basis that, the reaction rate increases on increasing the concentration of dye, as more number of molecules of dyes were available but a further increase in

concentration beyond 10×10^{-5} M results in an internal filter effect which does not permit sufficient amount of light to reach the surface of the photocatalyst thus, decreasing the rate of photocatalytic degradation of nigrosine.

Effect of amount of catalyst

The effect of variation of amount of catalyst on the rate of dye degradation has been observed in the range from 0.02g to 0.10g keeping other parameters identical. It has been seen that with an increase in the amount of catalyst, the rate of degradation increases to a certain amount of catalyst $\text{La}_2\text{Ce}_2\text{O}_7$ that is 0.08g. Beyond this limit, the rate of reaction becomes almost constant with any increase in amount of catalyst.

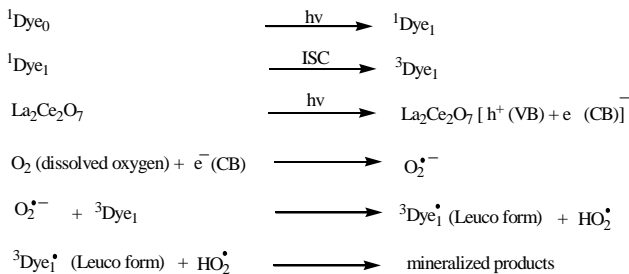
This may be explained by the fact that with an increase in the amount of catalyst, the surface area of catalyst will also increase. Hence, the rise in the rate of reaction has been observed. But for further increase in the amount of catalyst beyond a limit (0.08g), only the thickness of the layer (and not the exposed surface area) will increase at the bottom of reaction vessel, which was completely covered by the catalyst. It may be considered like a saturation point, above which any increase in the amount of catalyst has negligible or no effect on the rate of catalytic degradation of nigrosine.

Effect of Light Intensity

The effect of light intensity on rate of degradation of dye was also studied keeping all other parameters identical. The effect of light intensity on the rate of degradation of nigrosine was also studied by varying the intensity of light from 10.0 to 70.0 mWcm^{-2} . The results indicate that with increasing light intensity, the rate of reaction increases and maximum rates were found at 60.0 mWcm^{-2} . It can be explained on the basis that as the intensity of light was increased, the number of photons striking per unit area also increases, resulting into higher rate of degradation for dye. Further increase in the intensity of light above 60.0 mWcm^{-2} may start some side thermal reactions and hence, higher light intensities have been avoided.

Mechanism

On the basis of the experimental observations, a tentative mechanism has been proposed for the photocatalytic degradation (mineralization) of nigrosine in the presence of $\text{La}_2\text{Ce}_2\text{O}_7$.



Nigrosine dye absorbs radiations of suitable wavelength and gives rise to its excited singlet state. Then it undergoes intersystem crossing (ISC) to give the triplet state of the dye. On the other hand, the semiconductor ($\text{La}_2\text{Ce}_2\text{O}_7$) also absorbs light to excite an electron from its valence band (VB) to its conduction band (CB), leaving behind a hole in the valence band. This electron from the conduction band will be abstracted by oxygen molecule (dissolved oxygen) generating superoxide anion radical ($\text{O}_2^{\cdot-}$). Oxygen anion radical abstract a proton from triplet state of dye and is converted into dye radical and this radical is relatively unstable and degrades into some harmless smaller fragments (H_2O , CO_2).

The participation of $\text{O}_2^{\cdot-}$ and HO_2^{\cdot} radicals were considered as an oxidant species, because it was observed that reaction rate for degradation of nigrosine is not affected by the presence of $\cdot\text{OH}$ radical scavenger, isopropanol, which indicates $\cdot\text{OH}$ radicals are not playing any role in this degradation as an active oxidizing species in this reaction.

Adsorption of nigrosine dye on lanthanum cerate during degradation

It has been observed visually that during photocatalytic degradation, some amount of dye gets also adsorbed on the catalyst surface. Due to the adsorption of nigrosine on the catalyst surface, the color of the catalyst becomes black from original dull white color at the end of degradation process. It has been observed that adsorption of dye on catalyst surface started only in later stage of degradation. Initially, only decrease in absorbance due to photocatalytic degradation has been observed. In an attempt to isolate dye from the catalyst, a viscous substance was formed from which dye could not be separated. Conclusively lanthanum cerate removed the nigrosine dye from its aqueous solution both by photocatalytic degradation and adsorption.

Water quality parameters

Quality parameters of dye solution of nigrosine has been tested before and after its photocatalytic

degradation by measuring some parameters like COD, DO, conductance, salinity, TDS and pH. The results are summarized in Table 2.

Chemical Oxygen Demand (COD)

The mineralization of nigrosine was confirmed by measuring the decrease of COD value. COD of nigrosine dye solution was estimated before and after the photocatalytic treatment and the photodegradation efficiency of the catalyst was calculated from the following expression:

$$\eta = \frac{\text{COD}_{\text{before}} - \text{COD}_{\text{after}}}{\text{COD}_{\text{before}}} \times 100$$

η = Photodegradation efficiency (%),

$\text{COD}_{\text{before}}$ = COD of dye solution before exposure of light and

$\text{COD}_{\text{after}}$ = COD of dye solution after exposure of light

COD of dye solution before and after exposure of light has been determined by redox method. The photodegradation efficiency after 2 hours of exposure of light on nigrosine using nanoparticles of $\text{La}_2\text{Ce}_2\text{O}_7$ photocatalyst was found to be 78.87%.

Dissolved Oxygen (DO)

DO analysis measures the amount of gaseous oxygen dissolved in aqueous solution. Increase in dissolved oxygen (from 3.9 ppm to 4.4 ppm) after photocatalytic degradation of the dye indicates mineralization of dye to a significant extent.

Conductance, Salinity and Total dissolved solids (TDS)

Conductivity as a summation parameter is a measure of the level of ionic concentration of solution. Conductivity parameter has been increased after the treatment because dye has been mineralized into ions like CO_3^{2-} , NO_3^- , and SO_4^{2-} ions etc. Because of this reason, TDS and salinity of the dye solution was also found greater after photocatalytic degradation of dye.

Table 2 – Water quality parameters

Various parameters studied	Before photocatalytic degradation	After photocatalytic degradation
COD (mg/L)	43.36	9.16
DO (ppm)	3.9	4.4
Conductance (μS)	22.4	164
Salinity (ppt)	0.03	0.24
TDS (ppm)	12.1	81.8
pH	8.0	6.81

pH

It has been observed that initial pH of 8.0 has been decreased to 6.81 that is almost neutral pH after photocatalytic degradation of nigrosine. This also indicates the mineralization of dye after treatment.

Conclusion

Photocatalytic method is the most effective method for the treatment of wastewater. In the dark, the rate of photocatalytic reaction is slow, whereas on irradiation of reaction mixture with visible light, acceleration in the rate of degradation of nigrosine dye was observed. Lanthanum cerate has been prepared by citric acid assisted sol-gel method. The degradation occurs efficiently over a wide pH range of 5.0–9.0. Good degradation efficiency of nigrosine in aqueous solution (78.87%) was achieved within 2 h reaction time. At optimal conditions, rate of degradation of nigrosine dye was found to be $k = 3.38 \times 10^{-4} \text{ sec}^{-1}$. During photocatalytic process, $\text{O}_2^{\cdot-}$ radicals react with dye and degrade it into smaller products like H_2O , CO_2 , NO_3^- and SO_4^{2-} ions etc. The kinetics of the photodegradation in the presence of the nanocatalyst $\text{La}_2\text{Ce}_2\text{O}_7$ follows pseudo first-order rate model. Radical mechanism for degradation has been confirmed by using radical scavenger isopropanol.

Acknowledgement

The author (Nutan Salvi) is thankful to University Grants Commission (Rajiv Gandhi National Fellowship), New Delhi for providing financial assistance in the form of SRF. Thanks are also due to Head, Department of Chemistry, and Head, Department of Physics M. L. S. University, Udaipur for providing necessary infrastructure facilities and for TG-DTA characterization, respectively. I am also thankful to SICART, Vallabh Vidyanagar, Anand and SAIF, Chandigarh, India for characterization of sample.

References

- Babic J & Pavko A, *Acta Chim Slov*, 54 (2007) 730.
- Blanquez P, Casas N, Font X, Gabarrell X, Sarra M, Caminal G & Vicent T, *Water Res*, 38 (2004) 2166.
- Borchert M & Libra J A, *Biotechnol Bioeng*, 3 (2001) 312.
- Hassler J W, *Activated Carbon*, (Chemical Publishing Co. Inc., New York, 1963)
- Poyatos J M, Munio M M, Almecija M C, Torres J C, Hontoria E & Osorio F, *Water Air Soil Pollut*, 205 (2010) 187.
- Ghiselli G, Jardim W F, Litter M I & Mansilla H D, *J Photochem Photobiol A*, 167 (2004) 59.
- Ntampeglitis K, Riga A, Karayannis V, Bontozoglou V & Papapolymerou G, *J Hazard*, 136 (2006) 75.
- Lopez A, Pagano M, Volpe A & Di Pinto C, *Chemosphere*, 54 (2004) 1005.
- Morais J L & Zamora P P, *J Hazard Mater*, 123 (2005) 181.
- Canizares P, Paz R, Saez C & Rodrigo M A, *J Environ Manage*, 90 (2009) 410.
- Zhu B & Zou L, *J Environ Manage*, 90 (2009) 3217.
- Meng W, Hu R, Yang J, Du Y, Li J & Wang H, *Chinese J Catal*, 37 (2016) 1283.
- Moafi H F, Zanjanchi M A & Shojaie A F, *J Nanosci Nanotechnol*, 14 (2014) 7139.
- Anandan S, Vinu A, Mori T, Gokulakrishnan N, Srinivasu P, Murugesan V & Ariga K, *Catal Commun*, 8 (2007) 1377.
- Siah W R, Roslan N A, Lintang H O, Shamsuddin M & Yuliaty L, *Adv Mater Res*, 1112 (2015) 168.
- Wang C, Zhu Q, Gu C, Luo X, Yu C & Wu M, *RSC Adv*, 6 (2016) 85852.
- Jose J, Paliwal M, Gupta N, Punjabi P B & Sharma V K, *Int J Chem Sci*, 6 (2008) 111.
- Zhou X D, Huebner W & Anderson H U, *Chem Mater*, 15 (2003) 378.
- Lopes F W B, de Souza C P, de Souza A M V, de Morais, J P Dallas & Gavarrri J R, *Hydrometallurgy*, 97 (2009) 167.
- Besikiotis V, Knee C S, Ahmed I, Haugrud R & Norby T, *Solid State Ion*, 228 (2012) 1.
- Wang Y, Wang C, Li C, Cheng Y L & Chi F, *Ceram Inter*, 40 (2014) 4305.
- Song Z H, Ge C X, Gang L, Li W X & Dan D X, *J Eur Ceram Soc*, 32 (2012) 3693.
- Salehi S & Fathi M G, *Ceram Int*, 36 (2010) 1659.
- Lin C K, Zhang C M & Lin J, *J Phys Chem C*, 111 (2007) 3300.
- Gedanken A, Reisfeld R, Sominski E, Koltypin Y, Palchik O, Panzer G, Gaft M & Minti H, *J Phys Chem B*, 104 (2000) 7057.
- Su C & Suarez D L, *Clays Clay Miner*, 6 (1997) 814.
- Ion ED, Malic B, Arcon I, Gomilsek J P, Kodre A & Kosec M, *J Eur Ceram Soc*, 30 (2010) 569.